Theoretical Performance Limits on Tropospheric Refractivity Estimation Using Point-to-Point Microwave Measurements

Joseph Tabrikian, *Senior Member, IEEE*, and Jeffrey L. Krolik, *Member, IEEE*

***Abstract*— Ducted propagation above the ocean surface can seriously impact shipboard radar and communications. Point-to-point microwave measurements have been proposed as a means of estimating tropospheric refractivity for the purposes of characterizing surface-based ducts. This paper addresses the theoretical performance of refractivity estimates that can be made by combining field measurements at different frequencies with prior statistics of refractivity variation. Parameterizing the refractivity profile using empirical orthogonal functions derived from a historical database, both Cramer–Rao performance bounds and the maximum *a posteriori* (MAP) estimate are discussed using coherent or incoherent signals. Results obtained using a realistic model of refractivity conditions off Southern California suggest that multifrequency propagation measurements can significantly improve the estimation of refractivity and propagation loss profiles.**

***Index Terms*— Microwave measurements, refractivity, tropospheric propagation.**

I. Introduction

THE vertical and horizontal refractivity profile in coastal regions determines, to a large extent, the performance of shipboard radar and communications systems. If the atmospheric conditions, particularly water-vapor spatial distribution, were known, numerical propagation models could be used for such purposes as predicting detection ranges, correcting altitude estimates, and estimating surface backscatter strength. Since direct measurement of atmospheric conditions is difficult and expensive, remote sensing by multiple point-to-point propagation loss measurements at different frequencies has been proposed as a means of synoptic monitoring of tropospheric refractivity. The effect of the variability of atmospheric refractivity on propagation estimates using real data profiles has been investigated in [10].

The objective of this paper is to examine the inverse problem of determining refractivity from propagation measurements. In order to estimate refractivity, a parameterization of the refractivity profile is required. In this paper, a parameterization based on the second-order statistics of historical refractivity measurements is proposed and then used to calculate fundamental performance bounds on the estimation of these refractivity parameters by microwave sensing techniques. Both coherent and incoherent signal models consisting of several discrete frequencies are considered.

A common tool for evaluating the performance of a parameter estimation algorithm is the Cramer–Rao lower bound (CRLB) [11]. The CRLB has been widely used for exploring fundamental performance limits in many different fields (see, e.g., [6], [7]). The use of the CRLB is usually justified by appealing to the property, which asserts that it can be closely approached by the maximum-likelihood estimator under asymptotic conditions, i.e., "sufficiently large" signal-to-noise ratio (SNR) and/or observation time. However, when prior statistical information on the unknown parameters is available, the Bayesian version of the bound [11] is potentially more appropriate. For cases where prior statistical information exists only for some of the unknown parameters, the hybrid CRLB based on the Bayesian CRLB has been proposed in [9]. The Bayesian and hybrid versions of the CRLB, however, do not always yield greatest lower bounds (i.e., "tight" bounds) even asymptotically. Tighter Bayesian bounds have thus been developed by Weiss–Weinstein [12], Ziv–Zakai [14], and more recently, a hybrid-type Barankin bound by Reuven and Messer [8]. However, calculation of these bounds involves an extremely large amount of computation, which makes them impractical for the refractivity estimation problem. Thus, in order to include the effect of *a priori* statistical knowledge in this paper, the performance of an optimal Bayesian estimator—the maximum *a posteriori* (MAP) method—is evaluated as an indicator of the limiting performance.

The remainder of this paper is organized as follows. In Section II, the problem is defined and formulated. In Section III, the hybrid CRLB for this problem is developed and it is shown why it is not a greatest lower bound, even asymptotically. In Section IV, the MAP estimator is presented and its performance is studied. Section V presents simulations which illustrate the expected performance of the MAP estimator for tropospheric refractivity estimation. The conclusions are presented in Section VI.

II. Refractivity Estimation Problem Formulation

A. Refractivity Parameterization

Parameterization of the refractivity profile is necessary in order to obtain the bound on the variance of estimation errors. While a trilinear profile has previously been used in refractivity

Manuscript received May 12, 1998; revised March 15, 1999. This work was supported by ONR and SPAWAR-SSC San Diego under contract N66001-92-D-0092, delivery order 91.

The authors are with the Department of Electrical and Computer Engineering, Duke University, Durham, NC 27708-0291 USA.

Publisher Item Identifier S 0018-926X(99)07069-6.

0018–926X/99$10.00 © 1999 IEEE

estimation, in order to include the effects of ducting, in this work, historical atmospheric sounding data are used to derive a basis in terms of empirical orthogonal functions (EOF's) [5] $\psi_m(z), m = 1, \cdots, M$. This leads to the following decomposition of the refractivity profile $n(z)$ as a function of height z

$$n(z) = m(z) + \Psi(z)\boldsymbol{g} \tag{1}$$

where the function $m(z)$ represents the known mean of the refractivity profile and $\Psi(z) = [\psi_1(z), \cdots, \psi_M(z)]$ is a row vector of EOF's. The unknown coefficient vector $\boldsymbol{g}$ is assumed to be a zero-mean random vector, which expresses the uncertainty in the refractivity profile. In this paper, $\boldsymbol{g}$ is assumed to be multivariate Gaussian distributed. Note that the Gaussian assumption ignores the higher order moments of $\boldsymbol{g}$, which may be relevant in some circumstances.

Sampling the refractivity profile of (1) at heights $z_1, \cdots, z_N$ the resulting N equations can be expressed in matrix notation as

$$\boldsymbol{n} = \boldsymbol{m} + \boldsymbol{\Psi}\boldsymbol{g} \tag{2}$$

where

$$\begin{aligned}\boldsymbol{n} &= [n(z_1), \cdots, n(z_N)]^T \\ \boldsymbol{m} &= [m(z_1), \cdots, m(z_N)]^T \\ \boldsymbol{\Psi} &= [\Psi^T(z_1), \cdots, \Psi^T(z_N)]^T\end{aligned}$$

and T stands for the transposition operation. The vector $\boldsymbol{g}$ expresses the variation of the refractivity from the mean $\boldsymbol{m}$ along different basis vectors corresponding to the columns of the matrix $\boldsymbol{\Psi}$.

Using the above parameterization, estimating the refractivity profile can be performed by estimating the vector $\boldsymbol{g}$. In order to obtain prior statistics on the random parameter $\boldsymbol{g}$, at least M independent measurements of the refractivity profile are needed. Using a set of M historical refractivity profiles sampled at N heights denoted $\{\boldsymbol{n}_m\}_{m=1}^M$, the mean and covariance matrix of $\boldsymbol{n}$ can be approximated by

$$\boldsymbol{m} = E(\boldsymbol{n}) \approx \frac{1}{M}\sum_{m=1}^{M}\boldsymbol{n}_m \tag{3}$$

$$\boldsymbol{C}_n \triangleq \operatorname{cov}(\boldsymbol{n}) \approx \frac{1}{M}\sum_{m=1}^{M}(\boldsymbol{n}_m - \boldsymbol{m})(\boldsymbol{n}_m - \boldsymbol{m})^H \tag{4}$$

where H is the Hermitian transpose. The matrix $\boldsymbol{\Psi}$ can be obtained by singular value decomposition of $\boldsymbol{C}_n$

$$\boldsymbol{C}_n = \boldsymbol{\Psi}\boldsymbol{C}_g\boldsymbol{\Psi}^T. \tag{5}$$

This process also provides the second-order statistical information on the vector $\boldsymbol{g}$, $\boldsymbol{C}_g$. By definition, the matrix $\boldsymbol{C}_g$ is diagonal implying that the elements of $\boldsymbol{g}$ are statistically uncorrelated. Knowledge of the prior distribution of the unknown parameters is important in the estimation process and is used as an *a priori* distribution in the calculation of the hybrid bound as well as MAP estimate.

B. Measurement Model

In order to estimate the refractivity profile, the electromagnetic field at different frequencies is sampled at N points in space. Consider the following measurement model for a signal composed of L different discrete frequencies:

$$\boldsymbol{y}_l = \boldsymbol{a}_l(r, z, \boldsymbol{g})s_l(\boldsymbol{\theta}_l) + \boldsymbol{\eta}_l, \qquad l = 1, \cdots, L \tag{6}$$

where $\boldsymbol{y}_l$ is $N \times 1$ vector representing the complex envelope of the measured signal by the different sensors at frequency f_l and $s_l(\boldsymbol{\theta}_l)$ is the complex envelope of the signal at frequency f_l with unknown phase θ_l. The additive measurement noise $\boldsymbol{\eta}_l$ is a zero-mean Gaussian vector with covariance matrix $\boldsymbol{R}_\eta = \sigma^2\boldsymbol{I}$, where $\boldsymbol{I}$ is an identity matrix of size NL—the number of sensors times the number of frequencies. The vector $\boldsymbol{a}_l(\cdot,\cdot,\cdot)$ is a known vector function representing the field as a function of the sensor range r, height z, and the unknown refractivity vector parameter $\boldsymbol{g}$. The vector function $\boldsymbol{a}_l(\cdot,\cdot,\cdot)$ can be determined using a full-field numerical propagation model such as the radio physical optics (RPO) code [3]. The signal amplitude is known except the parameter $\boldsymbol{\theta}_l$, which represents the phase of the lth frequency. Defining

$$\begin{aligned}\boldsymbol{y} &\triangleq [\boldsymbol{y}_1^T, \cdots, \boldsymbol{y}_L^T]^T \\ \boldsymbol{\Theta} &\triangleq [\boldsymbol{\theta}_1, \cdots, \boldsymbol{\theta}_L]^T \\ \boldsymbol{s}(\boldsymbol{\Theta}) &\triangleq [s_1(\boldsymbol{\theta}_1), \cdots, s_L(\boldsymbol{\theta}_L)]^T \\ \boldsymbol{\eta} &\triangleq [\boldsymbol{\eta}_1^T, \cdots, \boldsymbol{\eta}_L^T]^T\end{aligned}$$

and

$$\boldsymbol{A}(r, z, \boldsymbol{g}) \triangleq \begin{bmatrix} \boldsymbol{a}_1(r,z,\boldsymbol{g}) & \boldsymbol{0} & \boldsymbol{0} & \cdots\cdots & \boldsymbol{0} \\ \boldsymbol{0} & \boldsymbol{a}_2(r,z,\boldsymbol{g}) & \boldsymbol{0} & \cdots\cdots & \boldsymbol{0} \\ \vdots & \vdots & & & \vdots \\ \vdots & \vdots & & & \vdots \\ \boldsymbol{0} & \boldsymbol{0} & \cdots\cdots & \boldsymbol{0} & \boldsymbol{a}_L(r,z,\boldsymbol{g}) \end{bmatrix}$$

then (6) can be rewritten as

$$\boldsymbol{y} = \boldsymbol{A}(r, z, \boldsymbol{g})\boldsymbol{s}(\boldsymbol{\Theta}) + \boldsymbol{\eta}. \tag{7}$$

The problem addressed here is estimation of the refractivity profile parameters $\boldsymbol{g}$ using the measurements $\boldsymbol{y}$. The source location, defined by the parameters (r, z), is assumed to be known. In addition, prior statistical information on the vector parameter $\boldsymbol{g}$ is assumed available from historical profiles via the decomposition of (5). The vector of phases $\boldsymbol{\Theta}$ is a nuisance parameter.

Two different signal models are considered here. In the first, the signals at different frequencies are coherent and, therefore, the relative phases at different frequencies are assumed known. The reference phase $\boldsymbol{\theta}_1$, however, is assumed unknown. In the second case, the signal at different frequencies is incoherent and the nuisance parameters are $\boldsymbol{\Theta} = [\boldsymbol{\theta}_1, \cdots, \boldsymbol{\theta}_L]^T$. Note that in general, M unknown parameters in the vector $\boldsymbol{g}$ are required to perfectly represent the refractivity profiles of the historical data. However, according to the prior statistical information, the variance of the higher order terms of $\boldsymbol{g}$ are usually close to zero. Therefore, these terms can be assumed to be known

and the number of the unknown parameters to be estimated can be decreased to $M_0 \ll M$.

In the case of a single sensor, $N = 1$ and the vectors $\{\boldsymbol{a}_l\}_{l=1}^{L}$ are scalars. The block diagonal matrix $\boldsymbol{A}$ in (7) becomes diagonal such that

$$\boldsymbol{A}(r,z,\boldsymbol{g}) = \mathrm{diag}(\boldsymbol{b}(r,z,\boldsymbol{g})) \tag{8}$$

$$[\boldsymbol{b}(r,z,\boldsymbol{g})]_l = a_l(r,z,\boldsymbol{g}), \qquad l = 1,\cdots,L. \tag{9}$$

Focusing in this paper on the case of a single source-receiver pair, the measurements can thus be formulated as

$$\boldsymbol{y} = \boldsymbol{h}_{r,z}(\boldsymbol{\alpha}) + \boldsymbol{\eta}. \tag{10}$$

The vector $\boldsymbol{\alpha}$ is defined as $\boldsymbol{\alpha} \triangleq [\boldsymbol{g}^T, \boldsymbol{\Theta}^T]^T$, and the elements of $\boldsymbol{h}_{r,z}(\boldsymbol{\alpha})$ are given by

$$[\boldsymbol{h}_{r,z}(\boldsymbol{\alpha})]_l \triangleq |s_l|[\boldsymbol{b}(r,z,\boldsymbol{g})]_l e^{j\boldsymbol{\theta}_l} \qquad l = 1,\cdots,L. \tag{11}$$

In the above model, the parameter of interest $\boldsymbol{g}$ is unknown random, while the unknown nuisance parameter $\boldsymbol{\Theta}$ is deterministic. In the following sections, the hybrid CRLB and performance of the MAP estimator for this model will be discussed.

III. Hybrid CRLB

In order to account for prior statistical information on some but not all the parameters, the hybrid form of Cramer–Rao bound has previously been proposed [9], [11]. The expression for the hybrid CRLB on the vector $\boldsymbol{g}$ is

$$\mathrm{cov}(\boldsymbol{g},\boldsymbol{\Theta}) \geq (E_{\boldsymbol{g}}[\boldsymbol{J}_1(\boldsymbol{g},\boldsymbol{\Theta})] + \boldsymbol{J}_2)^{-1} \tag{12}$$

where $\boldsymbol{J}_1(\boldsymbol{g},\boldsymbol{\Theta})$ is the Fisher information matrix (FIM) of $\boldsymbol{\alpha} \triangleq (\boldsymbol{g},\boldsymbol{\Theta})$ using the measurements $\boldsymbol{y}$

$$[\boldsymbol{J}_1(\boldsymbol{\alpha})]_{ij} = E_{\boldsymbol{y}|\boldsymbol{\alpha}}\left\{\frac{\partial \ln f(\boldsymbol{y}|\boldsymbol{\alpha})}{\partial \boldsymbol{\alpha}_i}\frac{\partial \ln f(\boldsymbol{y}|\boldsymbol{\alpha})}{\partial \boldsymbol{\alpha}_j}\right\} \tag{13}$$

and the matrix $\boldsymbol{J}_2$ stands for the FIM of the vector $\boldsymbol{g}$ based on its prior statistical information. The function $f(\boldsymbol{y}|\boldsymbol{\alpha})$ denotes the conditional probability density of the vector $\boldsymbol{y}$ given the vector parameter $\boldsymbol{\alpha}$.

The use of prior statistical information is important in the refractivity estimation problem because the matrix $\boldsymbol{J}_1$ is singular when the number of complex measurements is less than the half the number of unknown parameters. This implies the conventional CRLB goes to infinity, indicating an inability to estimate the desired parameters using the measurements only. Adding the prior statistical information, through the matrix $\boldsymbol{J}_2$, however, assures a finite bound at any SNR or number of measurements. Calculation of this bound, however, requires an expectation over $\boldsymbol{J}_1$ with respect to the random refractivity parameters, $\boldsymbol{g}$. The expectation can be approximated by averaging $\boldsymbol{J}_1$ for different realizations of the refractivity profiles obtained from historical refractivity data.

To evaluate the hybrid CRLB for refractivity estimation with coherent signals, the unknown vector includes one nuisance parameter θ_1 in addition to M_0 elements of $\boldsymbol{g}$. The ijth element of the matrix $\boldsymbol{J}_1$ for the coherent case is thus given by

$$\{\boldsymbol{J}_1\}_{ij} = \frac{2\boldsymbol{s}^H\boldsymbol{s}}{\sigma^2}\,\mathrm{Re}\begin{bmatrix} \dfrac{\partial \boldsymbol{b}^H}{\partial \boldsymbol{g}}\dfrac{\partial \boldsymbol{b}}{\partial \boldsymbol{g}} & j\dfrac{\partial \boldsymbol{b}^H}{\partial \boldsymbol{g}}\boldsymbol{b} \\ -j\boldsymbol{b}^H\dfrac{\partial \boldsymbol{b}}{\partial \boldsymbol{g}} & |\boldsymbol{b}|^2 \end{bmatrix} \tag{14}$$

since θ_1 cancels out. In the incoherent case, the unknown vector includes L nuisance parameters in addition to the M_0 elements of $\boldsymbol{g}$. The ijth element of the matrix $\boldsymbol{J}_1$ is given by (15), shown at the bottom of the page. Note that in both cases, the matrix $\boldsymbol{J}_1$ is independent of the phase vector $\boldsymbol{\Theta}$ since the dependence on the signal phase disappears in the product $\boldsymbol{s}^H\boldsymbol{s}$. The expression $\boldsymbol{s}^H\boldsymbol{s}/\sigma^2$ in (15) is defined here as the SNR.

The matrix $\boldsymbol{J}_2$ contains the *a priori* covariance matrix of the unknown parameter vector. The covariance matrix of the vector $\boldsymbol{g}$ can be calculated as described in Section II-A and is given by the diagonal matrix $\boldsymbol{C}_g$. Since for both coherent and incoherent signals no prior information on the nuisance vector parameter $\boldsymbol{\Theta}$ is available, it must be treated as unknown deterministic and the matrix $\boldsymbol{J}_2$ is given by (see [9])

$$\boldsymbol{J}_2 = \begin{bmatrix} \boldsymbol{C}_g & \boldsymbol{0} \\ \boldsymbol{0} & \boldsymbol{0} \end{bmatrix} \tag{16}$$

where the sizes of the zero matrices are determined by the number of unknown phase parameters in each case.

The CRLB is known to be an asymptotically greatest lower bound and it can be achieved by the maximum-likelihood estimator. The Bayesian CRLB on the other hand is not a tight bound even asymptotically [1]. The condition under which the Bayesian version of the CRLB can be achieved by some estimator is (see [11])

$$\frac{\partial \ln(f(\boldsymbol{y},\boldsymbol{\alpha}))}{\partial \boldsymbol{\alpha}} = \hat{\boldsymbol{\alpha}}(\boldsymbol{y}) - \boldsymbol{\alpha}, \quad \forall\, \boldsymbol{y},\boldsymbol{\alpha} \tag{17}$$

where $\hat{\alpha}(\boldsymbol{y})$ is an unbiased estimate of α which achieves the bound. Note that $f(\boldsymbol{y},\boldsymbol{\alpha})$ denotes the joint probability density

$$\{\boldsymbol{J}_1\}_{ij} = \frac{2\boldsymbol{s}^H\boldsymbol{s}}{\sigma^2}\mathrm{Re}\begin{bmatrix} \dfrac{\partial \boldsymbol{b}^H}{\partial \boldsymbol{g}}\dfrac{\partial \boldsymbol{b}}{\partial \boldsymbol{g}} & j\begin{bmatrix} \dfrac{\partial b_1^*}{\partial \boldsymbol{g}}b_1 & & \boldsymbol{0} \\ & \ddots & \\ \boldsymbol{0} & & \dfrac{\partial b_L^*}{\partial \boldsymbol{g}}b_L \end{bmatrix} \\ -j\begin{bmatrix} b_1^*\dfrac{\partial b_1}{\partial \boldsymbol{g}} & & \boldsymbol{0} \\ & \ddots & \\ \boldsymbol{0} & & b_L^*\dfrac{\partial b_L}{\partial \boldsymbol{g}} \end{bmatrix} & \begin{bmatrix} |b_1|^2 & & \boldsymbol{0} \\ & \ddots & \\ \boldsymbol{0} & & |b_L|^2 \end{bmatrix} \end{bmatrix} \tag{15}$$

function of $\boldsymbol{y}$ and $\boldsymbol{\alpha}$. Such a condition is not satisfied in general cases and, thus, the bound is usually unachievable. Therefore, the hybrid CRLB is usually not tight, even asymptotically.

If the matrix $\boldsymbol{J}_1$ is singular, then by increasing the SNR to infinity, only the nonzero eigenvalues of $\boldsymbol{J}_1$ go to infinity while other eigenvalues remain zero. Therefore, adding the prior statistical information, which does not vary with SNR, is expected to result in a constant error covariance as the SNR goes to infinity. However, in the refractivity estimation problem where $\boldsymbol{J}_1$ is singular, the hybrid CRLB leads to the unrealistic conclusion that the mean-square error of the refractivity estimation may go to zero as SNR goes to infinity even when $\boldsymbol{J}_1$ is singular. The reason is that the expectation over the matrix $\boldsymbol{J}_1$ with respect to the unknown random parameters makes it nonsingular. Thus, although the matrix $\boldsymbol{J}_1$ is singular for any value of the unknown parameters, its expected value with respect to the unknown random parameters is a nonsingular matrix whose eigenvalues increase with SNR. At high SNR's, the matrix $\boldsymbol{J}_2$ becomes negligible with respect to $E_{\boldsymbol{g}}[\boldsymbol{J}_1(\boldsymbol{g},\boldsymbol{\Theta})]$ and, therefore, the bound on error covariance is approximated by $E_{\boldsymbol{g}}^{-1}[\boldsymbol{J}_1(\boldsymbol{g},\boldsymbol{\Theta})]$. This matrix is inversely proportional to SNR and thus goes to zero as SNR goes to infinity. Thus, the hybrid CRLB is not a useful tool for prediction of performance limits in the refractivity estimation problem.

IV. Maximum *A Posteriori* Estimator Performance Analysis

Since, as discussed in the previous section, the Bayesian CRLB can be expected to provide only a weak indication of refractivity estimation performance, in this section, the performance of the optimal MAP estimator of the refractivity parameters is examined. To derive the performance of a general MAP estimator, consider the following measurement model:

$$\boldsymbol{y} = \boldsymbol{h}(\boldsymbol{\alpha})|_{\alpha=\alpha_o} + \boldsymbol{\eta} \tag{18}$$

and let $\boldsymbol{\alpha}_o$ denote the true vector parameter to be estimated. The MAP estimator of the vector parameter $\boldsymbol{\alpha}_o$ given the measurement vector $\boldsymbol{y}$ is

$$\hat{\boldsymbol{\alpha}}_{MAP}(\boldsymbol{y}) = \arg \max_{\boldsymbol{\alpha}} f(\boldsymbol{y},\boldsymbol{\alpha}) \tag{19}$$

where $f(\boldsymbol{y},\boldsymbol{\alpha})$ is the joint probability density function of the measurement vector $\boldsymbol{y}$ and the parameter vector $\boldsymbol{\alpha}$. Of interest here is the error around the true value of $\boldsymbol{\alpha}$. Note that the MAP estimator can also be written as

$$\hat{\boldsymbol{\alpha}}_{\mathrm{MAP}}(\boldsymbol{y}) = \arg \max_{\boldsymbol{\alpha}} u(\boldsymbol{y},\boldsymbol{\alpha}) \tag{20}$$

where $u(\boldsymbol{y},\boldsymbol{\alpha})$ is defined as

$$u(\boldsymbol{y},\boldsymbol{\alpha}) \triangleq \ln f(\boldsymbol{y}|\boldsymbol{\alpha}) + \ln f(\boldsymbol{\alpha}). \tag{21}$$

The goal here is to calculate the statistics of estimates of the parameter of interest $\boldsymbol{\alpha}$, assuming small errors in the neighborhood of α_o. For this purpose, the relation between small errors in the data $\boldsymbol{y}$ and estimate of $\boldsymbol{\alpha}_o$ is derived.

The MAP estimate of $\boldsymbol{\alpha}$ maximizes the function $u(\boldsymbol{y},\boldsymbol{\alpha})$ for a given measurement vector $\boldsymbol{y}$. Therefore, the gradient of $u(\boldsymbol{y},\boldsymbol{\alpha})$ with respect to $\boldsymbol{\alpha}$ is zero at $\hat{\boldsymbol{\alpha}}_{MAP}(\boldsymbol{y})$

$$\boldsymbol{u}_{\alpha}^{H}(\boldsymbol{y},\hat{\boldsymbol{\alpha}}_{\mathrm{MAP}}) = \boldsymbol{0} \tag{22}$$

where $\boldsymbol{u}_{\alpha}(\cdot,\cdot)$ is a row vector whose elements are the derivatives of $u(\cdot,\cdot)$ with respect to the elements in the row vector $\boldsymbol{\alpha}$

$$\boldsymbol{u}_{\alpha}(\boldsymbol{y},\boldsymbol{\alpha}) \triangleq \frac{\partial u(\boldsymbol{y},\boldsymbol{\alpha})}{\partial \boldsymbol{\alpha}}. \tag{23}$$

Let $\Delta\boldsymbol{\alpha}$ denote the estimation error of $\boldsymbol{\alpha}$:$\Delta\boldsymbol{\alpha} = \hat{\boldsymbol{\alpha}}_{\mathrm{MAP}} - \boldsymbol{\alpha}_o$. Substitution of (18) into (22) and expanding the Taylor series to first order gives

$$\begin{aligned}
&\boldsymbol{u}_{\alpha}^{H}(\boldsymbol{y},\hat{\boldsymbol{\alpha}}_{\mathrm{MAP}}) \\
&\quad = \boldsymbol{u}_{\alpha}^{H}(\boldsymbol{h}(\boldsymbol{\alpha}_o)+\boldsymbol{\eta},\boldsymbol{\alpha}_o+\Delta\boldsymbol{\alpha}) \\
&\quad = \boldsymbol{u}_{\alpha}^{H}(\boldsymbol{h}(\boldsymbol{\alpha}_o),\boldsymbol{\alpha}_o) \\
&\qquad + \left\{ \frac{\partial \boldsymbol{u}_{\alpha}(\boldsymbol{y},\boldsymbol{\alpha})}{\partial \boldsymbol{y}}\,\boldsymbol{\eta} + \frac{\partial \boldsymbol{u}_{\alpha}(\boldsymbol{y},\boldsymbol{\alpha})}{\partial \boldsymbol{\alpha}}\,\Delta\boldsymbol{\alpha} \right\}_{\substack{\boldsymbol{y}=\boldsymbol{h}(\boldsymbol{\alpha}_o)\\ \boldsymbol{\alpha}=\boldsymbol{\alpha}_o}} = \boldsymbol{0}
\end{aligned} \tag{24}$$

where

$$\left[\frac{\partial \boldsymbol{u}_{\alpha}(\boldsymbol{y},\boldsymbol{\alpha})}{\partial \boldsymbol{y}}\right]_{ij} \triangleq \frac{\partial^2 u(\boldsymbol{y},\boldsymbol{\alpha})}{\partial \alpha_i \partial \boldsymbol{y}_j}$$

$$\left[\frac{\partial \boldsymbol{u}_{\alpha}(\boldsymbol{y},\boldsymbol{\alpha})}{\partial \boldsymbol{\alpha}}\right]_{ij} \triangleq \frac{\partial^2 u(\boldsymbol{y},\boldsymbol{\alpha})}{\partial \alpha_i \partial \alpha_j}.$$

To evaluate (24), considering the derivatives with respect to $\boldsymbol{\alpha}$ at the true value of $\boldsymbol{\alpha}$, i.e., $\boldsymbol{y} = \boldsymbol{h}(\boldsymbol{\alpha}_o)$, $\boldsymbol{\alpha} = \boldsymbol{\alpha}_o$ achieves the maximum of $\ln f(\boldsymbol{y}|\boldsymbol{\alpha})$

$$\left.\frac{\partial \ln f(\boldsymbol{y}|\boldsymbol{\alpha})}{\partial \boldsymbol{\alpha}}\right|_{\substack{\boldsymbol{y}=\boldsymbol{h}(\boldsymbol{\alpha}_o)\\ \boldsymbol{\alpha}=\boldsymbol{\alpha}_o}} = \boldsymbol{0}^{H}.$$

Therefore, the gradient of (21) with respect to $\boldsymbol{\alpha}$ is given by

$$\boldsymbol{u}_{\alpha}(\boldsymbol{h}(\alpha_o),\boldsymbol{\alpha}_o) = \left.\frac{\partial \ln f(\boldsymbol{\alpha})}{\partial \boldsymbol{\alpha}}\right|_{\boldsymbol{\alpha}=\boldsymbol{\alpha}_o} \tag{25}$$

and (24) can be written as

$$\left\{ \frac{\partial \ln f(\boldsymbol{\alpha})}{\partial \boldsymbol{\alpha}^H} + \frac{\partial \boldsymbol{u}_{\alpha}(\boldsymbol{y},\boldsymbol{\alpha})}{\partial \boldsymbol{y}}\boldsymbol{\eta} + \frac{\partial \boldsymbol{u}_{\alpha}(\boldsymbol{y},\boldsymbol{\alpha})}{\partial \boldsymbol{\alpha}}\,\Delta\boldsymbol{\alpha} \right\}_{\substack{\boldsymbol{y}=\boldsymbol{h}(\boldsymbol{\alpha}_o)\\ \boldsymbol{\alpha}=\boldsymbol{\alpha}_o}} = \boldsymbol{0}. \tag{26}$$

Therefore, the estimation error $\Delta\boldsymbol{\alpha}$ is approximately

$$\begin{aligned}
\Delta\boldsymbol{\alpha} = \Bigg\{ &-\left[\frac{\partial \boldsymbol{u}_{\alpha}(\boldsymbol{y},\boldsymbol{\alpha})}{\partial \boldsymbol{\alpha}}\right]^{-1} \\
&\cdot \left[\frac{\partial \ln f(\boldsymbol{\alpha})}{\partial \boldsymbol{\alpha}^H} + \frac{\partial \boldsymbol{u}_{\alpha}(\boldsymbol{y},\boldsymbol{\alpha})}{\partial \boldsymbol{y}}\boldsymbol{\eta}\right] \Bigg\}_{\substack{\boldsymbol{y}=\boldsymbol{h}(\boldsymbol{\alpha}_o)\\ \boldsymbol{\alpha}=\boldsymbol{\alpha}_o}}.
\end{aligned} \tag{27}$$

Equation (27) shows the relation between the additive noise $\boldsymbol{\eta}$ and the resulting errors in the estimation of $\boldsymbol{\alpha}$ for small errors and/or large SNR's. The above equations permits the

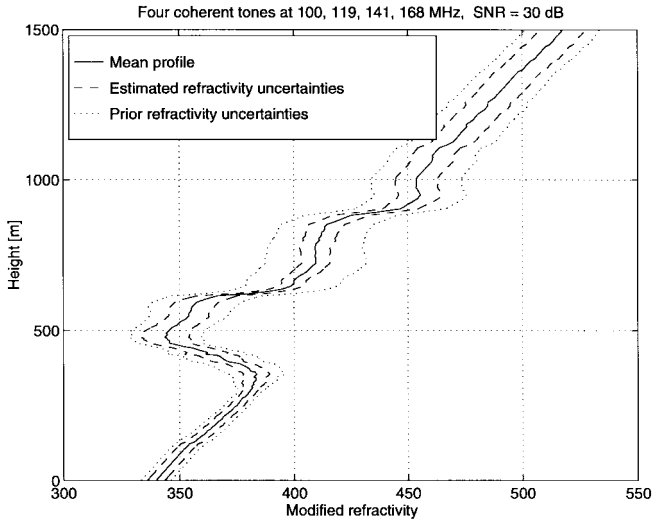

Fig. 1. The reference refractivity profile bracketed by curves, which are one STD away using coherent signals at four frequencies.

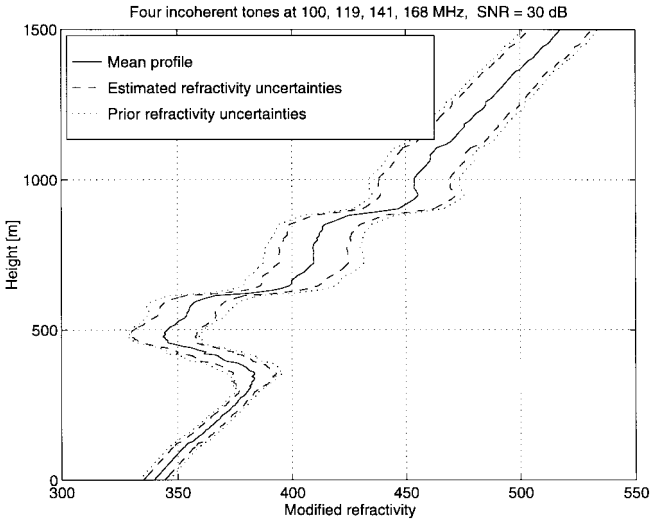

Fig. 2. The reference refractivity profile bracketed by curves, which are one STD away using incoherent signals at four frequencies.

derivation of the statistics of $\Delta\boldsymbol{\alpha}$ from probability density functions of $\boldsymbol{\eta}$ and $\boldsymbol{\alpha}$.

In order to compare the performance of the MAP estimator with the Bayesian CRLB, consider the case where the noise vector $\boldsymbol{\eta}$ and the unknown parameter $\boldsymbol{\alpha}$ are independent Gaussian vectors

$$\boldsymbol{\eta} \sim N(\mathbf{0}, \boldsymbol{R}_\eta)$$
$$\boldsymbol{\alpha} \sim N(\overline{\boldsymbol{\alpha}}, \boldsymbol{R}_\alpha).$$

For the model of (18) and this Gaussian assumption, the FIM's, $\boldsymbol{J}_1$, and $\boldsymbol{J}_2$ are given by

$$\boldsymbol{J}_1 = \left[\frac{\partial \boldsymbol{h}^H(\boldsymbol{\alpha})}{\partial \boldsymbol{\alpha}} \boldsymbol{R}_\eta^{-1} \frac{\partial \boldsymbol{h}(\boldsymbol{\alpha})}{\partial \boldsymbol{\alpha}}\right]_{\boldsymbol{\alpha}=\boldsymbol{\alpha}_o} \tag{28}$$

$$\boldsymbol{J}_2 = \boldsymbol{R}_\alpha^{-1}. \tag{29}$$

Using the expression in (27) under a Gaussian assumption, calculation of the gradient $\boldsymbol{u}_\alpha(\boldsymbol{y}, \boldsymbol{\alpha})$ is required. By substituting Gaussian density functions for the measurements $\boldsymbol{y}$ and the parameters $\boldsymbol{\alpha}$ into (21) one obtains

$$\boldsymbol{u}_\alpha(\boldsymbol{y}, \boldsymbol{\alpha}) = (\boldsymbol{y} - \boldsymbol{h}(\boldsymbol{\alpha}))^H \boldsymbol{R}_\eta^{-1} \frac{\partial \boldsymbol{h}(\boldsymbol{\alpha})}{\partial \boldsymbol{\alpha}} - (\boldsymbol{\alpha} - \overline{\boldsymbol{\alpha}})^H \boldsymbol{R}_\alpha^{-1}. \tag{30}$$

Using (30) and the prior density function of $\boldsymbol{\alpha}$, one may obtain the required terms for calculating $\Delta\boldsymbol{\alpha}$ in (27)

$$\left[\frac{\partial \boldsymbol{u}_\alpha(\boldsymbol{y}, \boldsymbol{\alpha})}{\partial \boldsymbol{y}}\right]_{\substack{\boldsymbol{y}=\boldsymbol{h}(\boldsymbol{\alpha}_o) \\ \boldsymbol{\alpha}=\boldsymbol{\alpha}_o}} = \left[\frac{\partial \boldsymbol{h}^H(\boldsymbol{\alpha})}{\partial \boldsymbol{\alpha}}\right]_{\boldsymbol{\alpha}=\boldsymbol{\alpha}_o} \boldsymbol{R}_\eta^{-1} \tag{31}$$

$$\begin{aligned}\left[\frac{\partial \boldsymbol{u}_\alpha(\boldsymbol{y}, \boldsymbol{\alpha})}{\partial \boldsymbol{\alpha}}\right]_{\substack{\boldsymbol{y}=\boldsymbol{h}(\boldsymbol{\alpha}_o) \\ \boldsymbol{\alpha}=\boldsymbol{\alpha}_o}} &= -\left[\frac{\partial \boldsymbol{h}^H(\boldsymbol{\alpha})}{\partial \boldsymbol{\alpha}} \boldsymbol{R}_\eta^{-1} \frac{\partial \boldsymbol{h}(\boldsymbol{\alpha})}{\partial \boldsymbol{\alpha}}\right]_{\boldsymbol{\alpha}=\boldsymbol{\alpha}_o} \\ &\quad - \boldsymbol{R}_\alpha^{-1} \\ &= -(\boldsymbol{J}_1(\boldsymbol{\alpha}_o) + \boldsymbol{J}_2) \end{aligned} \tag{32}$$

$$\left[\frac{\partial \ln f(\boldsymbol{\alpha})}{\partial \boldsymbol{\alpha}^H}\right]_{\boldsymbol{\alpha}=\boldsymbol{\alpha}_o} = \boldsymbol{R}_\alpha^{-1}(\overline{\boldsymbol{\alpha}} - \boldsymbol{\alpha}_o) = \boldsymbol{J}_2(\overline{\boldsymbol{\alpha}} - \boldsymbol{\alpha}_o). \tag{33}$$

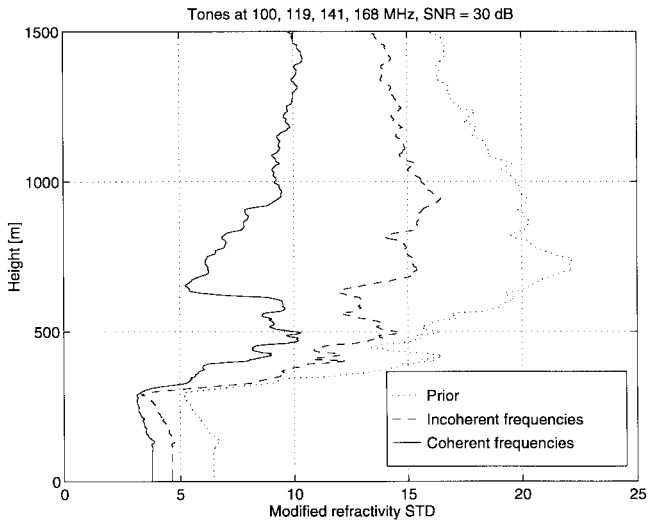

Fig. 3. The modified refractivity profile STD for prior information only and prior information in addition to measurements of coherent/incoherent signals.

Now, the MAP estimation error $\Delta\boldsymbol{\alpha}$ can be expressed as

$$\begin{aligned}\Delta\boldsymbol{\alpha} = &-(\boldsymbol{J}_1(\boldsymbol{\alpha}_o) + \boldsymbol{J}_2)^{-1} \\ &\cdot \left(\left[\frac{\partial \boldsymbol{h}^H(\boldsymbol{\alpha})}{\partial \boldsymbol{\alpha}}\right]_{\boldsymbol{\alpha}=\boldsymbol{\alpha}_o} \boldsymbol{R}_\eta^{-1}\boldsymbol{\eta} + \boldsymbol{J}_2(\overline{\boldsymbol{\alpha}} - \boldsymbol{\alpha}_o)\right).\end{aligned} \tag{34}$$

The bias of the estimator can be calculated by averaging the estimation error $\Delta\boldsymbol{\alpha}$: $\Delta\boldsymbol{\alpha}_b = E_{\boldsymbol{y}|\boldsymbol{\alpha}}(\Delta\boldsymbol{\alpha})$. The averaging operation results in

$$\Delta\boldsymbol{\alpha}_b = (\boldsymbol{J}_1(\boldsymbol{\alpha}_o) + \boldsymbol{J}_2)^{-1} \boldsymbol{J}_2(\overline{\boldsymbol{\alpha}} - \boldsymbol{\alpha}_o) \tag{35}$$

and the conditional mean-square error of the MAP estimator is

$$\begin{aligned}E_{\boldsymbol{y}|\boldsymbol{\alpha}}(\Delta\boldsymbol{\alpha}\Delta\boldsymbol{\alpha}^H|\boldsymbol{\alpha}) = &(\boldsymbol{J}_1(\boldsymbol{\alpha}) + \boldsymbol{J}_2)^{-1}(\boldsymbol{J}_1(\boldsymbol{\alpha}) + \boldsymbol{J}_2(\overline{\boldsymbol{\alpha}} - \boldsymbol{\alpha}) \\ &\cdot (\overline{\boldsymbol{\alpha}} - \boldsymbol{\alpha})^H \boldsymbol{J}_2)(\boldsymbol{J}_1(\boldsymbol{\alpha}) + \boldsymbol{J}_2)^{-1}.\end{aligned} \tag{36}$$

Thus, the global mean-square error of the MAP estimator is obtained by expectation of (36) with respect to $\boldsymbol{\alpha}$

$$\begin{aligned}E_{\boldsymbol{y},\boldsymbol{\alpha}}(\Delta\boldsymbol{\alpha}\Delta\boldsymbol{\alpha}^H) = &E_{\boldsymbol{\alpha}}((\boldsymbol{J}_1(\boldsymbol{\alpha}) + \boldsymbol{J}_2)^{-1}(\boldsymbol{J}_1(\boldsymbol{\alpha}) + \boldsymbol{J}_2(\overline{\boldsymbol{\alpha}} - \boldsymbol{\alpha}) \\ &\cdot (\overline{\boldsymbol{\alpha}} - \boldsymbol{\alpha})^H \boldsymbol{J}_2)(\boldsymbol{J}_1(\boldsymbol{\alpha}) + \boldsymbol{J}_2)^{-1}).\end{aligned} \tag{37}$$

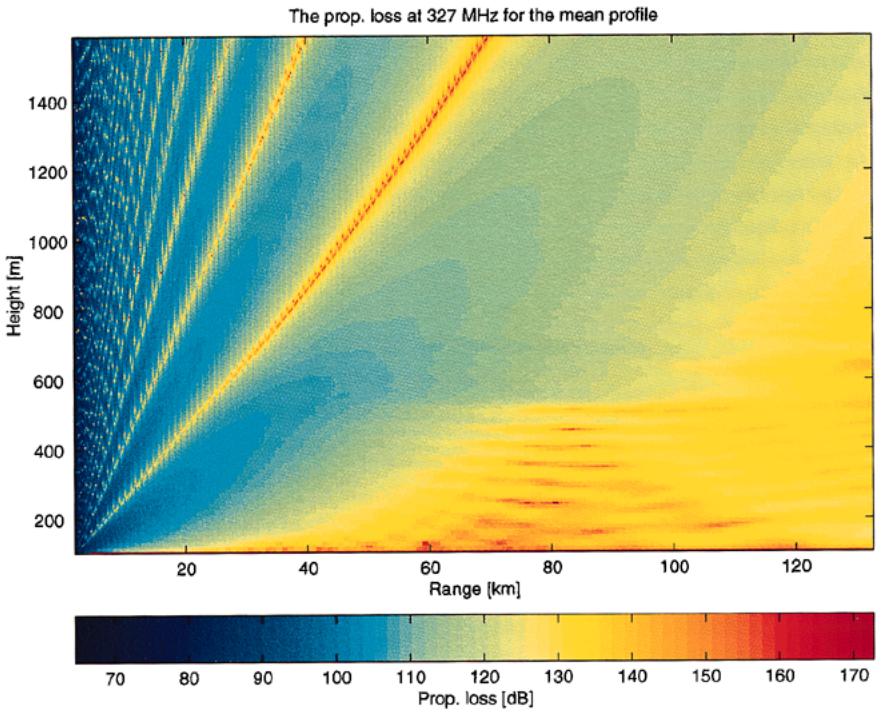

Fig. 4. The propagation loss for the mean profile.

In the special case where $\boldsymbol{J}_1$ is not a function of $\boldsymbol{\alpha}$, the mean-square error of the MAP estimator becomes

$$E_{\boldsymbol{y},\boldsymbol{\alpha}}(\Delta\boldsymbol{\alpha}\Delta\boldsymbol{\alpha}^H) = (\boldsymbol{J}_1 + \boldsymbol{J}_2)^{-1}. \tag{38}$$

This result coincides with the Bayesian CRLB (12) since $E_{\boldsymbol{\alpha}}(\boldsymbol{J}_1) = \boldsymbol{J}_1$. In other words, the MAP estimator is asymptotically optimal and achieves the CRLB in cases where $\boldsymbol{J}_1$ does not depend on α.

V. Estimation of Refractivity Estimator Performance

In this section, a performance evaluation of the MAP estimator of the modified refractivity profile [2], [4] is presented. The scenario considered here approximates that of the variability of coastal atmospheric refractivity (VOCAR) experiment described in [13]. A range independent propagation environment is considered. Measurements are assumed at a single receiver located at a height of 30.5 m and at a range of 132.6 km from the transmitter located at the same height. The sampling grid in height was chosen adaptively by RPO. The data model consists of four narrow-band signals at frequencies of 100, 119, 141, and 168 MHz. The number of EOF's, that is, the length of the uncertain vector, is chosen to be 20. Both the coherent case where the relative phase between the signals is known and the incoherent case where the relative phase is unknown were considered.

Prior statistics were estimated using real measurements of modified refractivity profiles taken during the VOCAR experiment. A total of 42 measured profiles were used in order to estimate the variance of the modified refractivity profile at different heights according to (3) and (4). Parameterization of the modified refractivity profile deviation was done using the decomposition in (5) from which the matrix $\boldsymbol{\Psi}$ is calculated. A typical profile was used as a reference profile around which the performance evaluation has been carried out. The performance evaluation has been made around this reference profile.

Using the equations developed in Section IV for $\boldsymbol{J}_1$, $\boldsymbol{J}_2$, and (37), the covariance matrix on estimation of the unknown, random refractivity parameter vector $\boldsymbol{g}$ is calculated. The expectation in (37) is approximated by averaging modified refractivity profiles from VOCAR data [13]. Given the covariance matrix on estimation error of the matrix $\boldsymbol{g}$, one may obtain the covariance matrix on estimation error of the modified refractivity profile $\boldsymbol{n}$ by using (5). In Fig. 1, the reference refractivity profile is plotted bracketed by curves that are one standard deviation (STD) away using: 1) only prior refractivity statistics and 2) a MAP estimate obtained using prior statistics together with field measurements made by the sensor assuming coherent signals at different frequencies. Clearly, with only the field measurements, as modeled by (7), one is not able to estimate the refractivity profile. However, such measurements combined with the prior refractivity parameter distribution can be used to significantly reduce the uncertainty in the profile. Fig. 2 shows the performance when incoherent signals at the four frequencies are used. Comparison of the standard deviations of the modified refractivity profile estimation for both coherent and incoherent signals versus that achieved using only the prior statistics is given in Fig. 3. In both coherent and incoherent cases, one can observe that a significant improvement in modified refractivity profile accuracy is obtained from the MAP estimate that uses field measurements.

The proposed technique for estimating the propagation loss can be applied at any frequency, regardless of the frequencies used to estimate the refractivity profile. In this model, the refractivity profile is estimated using coherent measurements

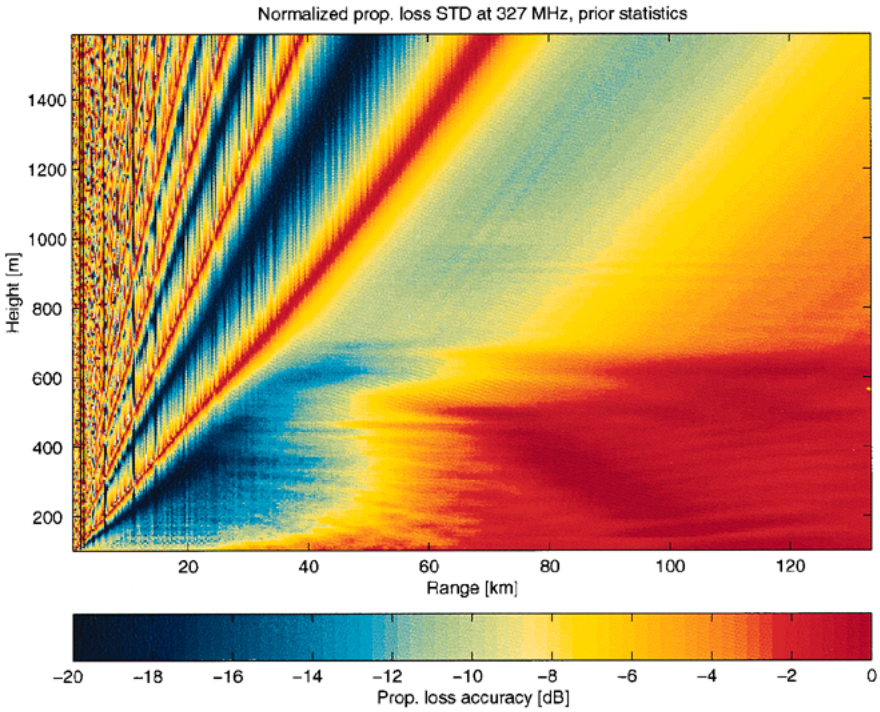

Fig. 5. Normalized STD of the propagation loss-prior statistics only.

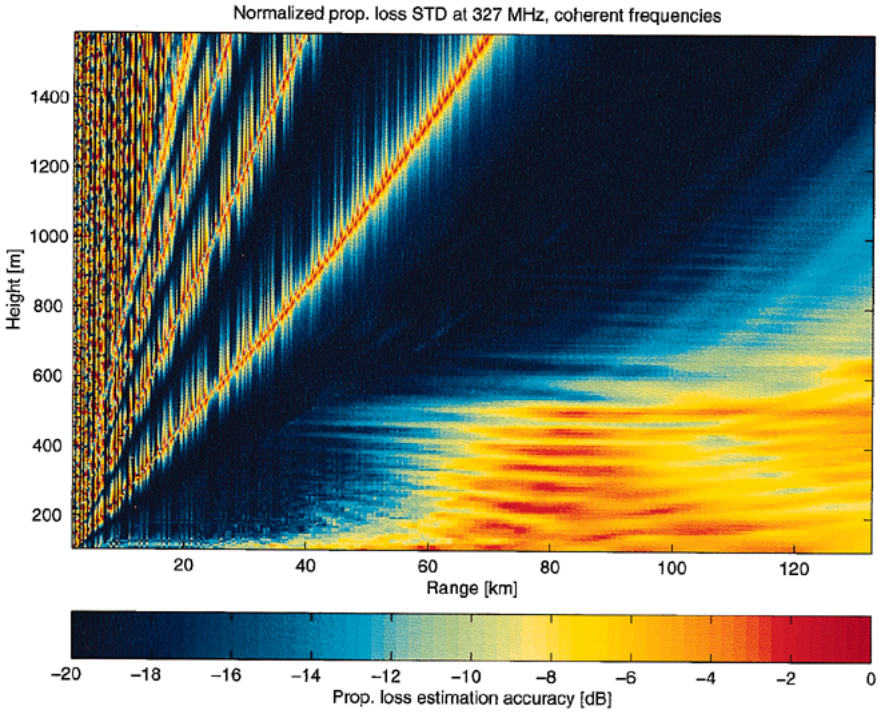

Fig. 6. Normalized STD of the propagation loss with estimation of the profile by four coherent frequencies.

at discrete frequencies 100, 119, 141, and 168 MHz, while the estimated refractivity profile is used to estimate the propagation loss at 327 MHz. The propagation loss was computed at a different frequency than those used to estimate refractivity to provide an indication of how useful the technique might be in applications where measurements cannot be collected at the frequency where propagation assessment is required. Fig. 4 shows the propagation loss for the mean profile as a function of range and height. The variance of the propagation loss estimates may be achieved using Monte-Carlo evaluation of a numerical propagation model for modified refractivity profiles distributed with covariance predicted by the bound of

(12). For this purpose, 100 realization of the electromagnetic field with independent randomization of the vector $\boldsymbol{g}$ according to its prior statistics. As previously assumed, the vector $\boldsymbol{g}$ is Gaussian. The normalized standard deviation (STD) of the propagation loss based on the prior information only versus prior information plus field measurements were evaluated and presented in Figs. 5 and 6, respectively. The normalized STD is defined as

$$\text{NSTD} \triangleq L_{\text{std}}/L_{\text{mean}}$$

where L_{std} is the STD of the propagation loss, and L_{mean} is the mean of the propagation loss. Comparison of Figs. 5 and 6 indicate that microwave remote sensing can very significantly improve the accuracy of propagation loss predictions. Fig. 5 shows that the NSTD around 100 km in low heights is about 0 dB, i.e., standard deviation of the propagation loss using no measurements is close to its mean. Fig. 6 shows that the STD of the estimated propagation loss in the same region can be reduced to -4 dB, i.e., an accuracy of 40% around the mean.

VI. Conclusions

In this paper, the problem of tropospheric refractivity measurements using remote microwave sensing technique has been addressed. It is shown that unlike the CRLB, the hybrid CRLB is in general not tight even asymptotically. Thus the MAP estimator is proposed for this problem and its performance has been analyzed and evaluated. Performance evaluation of the MAP estimator indicates that while prior statistics on refractivity alone yield poor predictions, the fusion of these statistics with a few propagation loss measurements can potentially predict propagation losses at different frequencies and spatial locations to within 10–60% of their true values at ranges out to 130 km in the UHF band.

Acknowledgment

The authors would like to thank T. Rogers for providing us with the VOCAR data as well as several useful discussions. In addition, they would like to thank O. Wüst for his contribution in porting the RPO code to our computers. The authors gratefully acknowledge the anonymous reviewers of this manuscript for their very helpful comments.

References

[1] B. Z. Bobrovsky, E. Mayer-Wolf, and M. Zakai, "Some classes of global Cramer–Rao bounds," *Ann. Stat.*, vol. 15, pp. 1421–1438, 1987.
[2] H. V. Hitney, "Refractive effects from VHF to EHF—Part A: Propagation mechanism," AGARD Lecture Ser. 196, Sept. 1994.
[3] ——, "Hybrid ray optics and parabolic equation methods for radar propagation modeling," in *Radar '92 Conf.*, Oct. 1992, pub. 365, pp. 58–61.
[4] D. E. Kerr, *Propagation of Short Radio Waves*. New York: McGraw-Hill, 1951.
[5] L. R. LeBlanc and F. H. Middleton, "An underwater acoustic sound velocity data model," *J. Acoust. Soc. Amer.*, vol. 67, pp. 2055–2062, 1980.
[6] S. Li and P. M. Schultheiss, "Depth measurement of remote sources using multipath propagation," *IEEE J. Oceanic Eng.*, vol. 18, pp. 379–387, July 1993.
[7] S. Narasimhan and J. L. Krolik, "Fundamental limits on acoustic source range estimation performance in uncertain ocean channels," *J. Acoust. Soc. Amer.*, vol. 97, no. 1, pp. 215–226, 1995.
[8] I. Reuven and H. Messer, "A Barankin-type lower bound on the estimation error of a hybrid parameter vector," *IEEE Trans. Inform. Theory*, vol. 43, pp. 1084–1093, May 1997.
[9] Y. Rockah and P. M. Schultheiss, "Array shape calibration using sources in unknown locations. I. Far-field sources, *IEEE Trans. Acoust., Speech Signal Processing*, vol. ASSP-35, pp. 286–299, Mar. 1987.
[10] T. Rogers, "Effects of the variability of atmospheric refractivity on propagation estimates," *IEEE Trans. Antennas Propagat.*, vol. AP-44, pp. 460–465, Apr. 1996.
[11] H. L. Van Trees, *Detection, Estimation and Modulation Theory*. New York: Wiley, 1968.
[12] A. Weiss and E. Weinstein, "A lower bound on the mean square error in random parameter estimation," *IEEE Trans. Inform. Theory*, vol. 31, pp. 680–682, 1985.
[13] R. A. Paulus, "An experiment in variability of coastal atmospheric refractivity," *Proc. Int. Geosci. Remote Sensing Symp. (IGRASS)*, Aug. 1994, vol. 1, pp. 386–388.
[14] J. Ziv and M. Zakai, "Some lower bounds on signal parameter estimation," *IEEE Trans. Inform. Theory*, vol. IT-15, pp. 386–391, May 1969.

Joseph Tabrikian (S'88–M'96–SM'98) received the B.Sc., M.Sc., and Ph.D. degrees in electrical engineering from Tel Aviv University, Israel, in 1986, 1992, and 1997, respectively.

From 1986 to 1991, he served as an electrical engineer in the Israeli Air Force, where he was involved in development of several projects of command and control systems and radar data analysis. From 1991 to 1996 he was a Teaching Assistant at the Department of Electrical Engineering Systems, Tel Aviv University. From September 1996 to October 1998 he was with the Department of Electrical and Computer Engineering, Duke University, Durham, NC, as a Research Assistant Professor. His research interests include source detection and localization, matched-field processing, and statistical signal analysis. He is currently a Faculty Member in the Department of Electrical and Computer Engineering, Ben-Gurion University, Beer-Sheba, Israel.

Jeffrey L. Krolik (M'86) was born in Canada. He received the Ph.D. degree in electrical engineering from the University of Toronto, ON, Canada, 1987.

He is an Associate Professor of Electrical and Computer Engineering at Duke University, Durham, NC. Between 1986 and 1990, he was an Assistant Professor of Electrical and Computer Engineering at Concordia University, Montreal. To pursue signal processing applications in the ocean sciences, he became an Assistant Research Scientist at the Scripps Institution of Oceanography, University of California, San Diego, in 1990. In 1992, he joined the faculty of Duke University. His research interests are in statistical signal and array processing with computational acoustic and electromagnetic models.

Dr. Krolik served as the Associate Editor of Acoustic Signal Processing, Journal of the Acoustical Society of America, from 1995 to 1998. He is currently a member of the Sensor and Multichannel Signal Processing technical committee of the IEEE SP Society.